

Evidence of a consolute critical point in the phase separation regime of $\text{La}_{5/8-y}\text{Pr}_y\text{Ca}_{3/8}\text{MnO}_3$ ($y \sim 0.4$) single crystals

G. Garbarino,¹ C. Acha,^{1,*} P. Levy,² T. Y. Koo,³ and S-W. Cheong⁴

¹Laboratorio de Bajas Temperaturas, Departamento de Física, FCEyN, Universidad de Buenos Aires, Ciudad Universitaria, (C1428EHA) Buenos Aires, Argentina

²Departamento de Física, CAC, Comisión Nacional de Energía Atómica, Gral Paz 1499, 1650 San Martín, Buenos Aires, Argentina

³Pohang Accelerator Laboratory, Pohang University of Science and Technology, Pohang, 790-784, South Korea

⁴Rutgers Center for Emergent Materials and Department of Physics and Astronomy, Rutgers University, Piscataway, New Jersey 08854, USA

(Received 31 March 2006; revised manuscript received 7 September 2006; published 25 September 2006)

We report on the dc and pulsed electric field sensitivity of the resistance of mixed valent Mn-oxide-based $\text{La}_{5/8-y}\text{Pr}_y\text{Ca}_{3/8}\text{MnO}_3$ ($y \sim 0.4$) single crystals as a function of temperature. The low-temperature regime of the resistivity is highly current and voltage dependent. An irreversible transition from high to low resistivity (LR) is obtained upon the increase of the electric field up to a temperature-dependent critical value (V_c). The current-voltage characteristics in the LR regime as well as the lack of a variation in the magnetization response when V_c is reached indicate the formation of a non-singly-connected filamentary conducting path. The obtained temperature dependence of V_c has a critical behavior similar to the one observed in binary liquid mixtures near their consolute point.

DOI: [10.1103/PhysRevB.74.100401](https://doi.org/10.1103/PhysRevB.74.100401)

PACS number(s): 75.40.-s, 72.20.Ht, 72.15.-v, 75.47.Lx

A controlled mixture of charge-delocalized ferromagnetic (CD-F) and charge-ordered antiferromagnetic (CO-AF) phases can be easily achieved in manganites that are in the phase separation (PS) regime. This was indeed observed in previous experiments in hole-doped manganites where the proportion of the CD-F phase was varied by changing temperature, electric or magnetic field, grain size, or solely by waiting for the evolution of the system to a different phase distribution.¹⁻⁵ Changes of several orders of magnitude were observed, for example, in the resistivity of the (La,Pr,Ca)MnO₃ compound, that were associated with the variation of the CD-F to CO-AF phase proportion, which determines the percolation scenario that governs the physics of this system.^{6,7} The study of the properties of the electric-field-dependent phase distribution may reveal the nature of some intrinsic attributes of these PS materials, like their topological phase distribution,⁸ their electrical transport mechanism,⁹ or their dynamical magnetic properties.¹⁰

In this paper we present the electric field sensitivity of resistivity and magnetization as a function of temperature in $\text{La}_{5/8-y}\text{Pr}_y\text{Ca}_{3/8}\text{MnO}_3$ ($y \sim 0.4$) (LPCMO) single crystals. We show that the two-phase percolation model, where the CD-F to CO-AF phase proportion increases as the applied electric field is increased, can only partially explain our results. A filamentary dielectric breakdown scenario gives instead a better understanding of the measured properties, where the observed critical behavior of the breakdown field points to the existence of a consolute point related to the separation of the CD-F and CO-AF phases. This similarity between binary liquid mixtures and magnetic phases in manganites can be useful to gain a deep understanding of the PS phenomena.

We have performed resistivity measurements as a function of temperature and electric field, $\rho(T, V)$, for temperatures in the $4 \leq T \leq 300$ K range, and electric fields up to 200 V cm^{-1} , in $\text{La}_{5/8-y}\text{Pr}_y\text{Ca}_{3/8}\text{MnO}_3$ ($y \sim 0.4$) single crystals. Details of their synthesis and characterization can be

found elsewhere.¹¹ Different contact configurations were used: a four-terminal (4W) standard configuration for constant current measurements and a two-wire (2W) configuration for high resistances (up to $100 \text{ G}\Omega$) or for a constant voltage measurement. We also performed pulsed current-voltage measurements (I - V characteristics), by generating a single square pulse of increasing voltage (up to 10 V) for 20 ms to 2 s . Temperature was measured by a small diode thermometer well thermally anchored to the sample. Most of the electrical transport experiments were performed without applying an external magnetic field. When small magnetic fields were applied ($H \sim 100 \text{ Oe}$), we followed a zero-field-cooled-warming (ZFCW) procedure. Magnetization measurements in ZFCW and field-cooled-cooling (FCC) modes were also performed as a function of temperature using a vibrating sample magnetometer. In order to estimate the variation of the ferromagnetic volume fraction upon the application of an increasing electric field, magnetization measurements at a fixed temperature (T_0) were also performed simultaneously with a $2W \rho(T_0, V)$ measurement.

Figure 1 and its inset show the resistivity of a LPCMO ($y \sim 0.4$) single crystal as a function of temperature for different constant currents and voltages (in the inset). For the low-voltage range ($V \leq 10 \text{ V}$), the sample remains insulating down to low temperatures. Saturation is observed most probably due to the fact that the resistivity of the sample is beyond our measurement capability. When higher voltages are applied ($10 \leq V \leq 100 \text{ V}$), a metal-insulator-like transition can be observed. A resistive drop of more than four orders of magnitude is obtained for the highest voltages as well as a characteristic temperature hysteresis for this system.⁷ A similar behavior is observed for the current controlled experiment.

Figure 2 shows the voltage dependence of the resistivity [$\rho(V)$, 2W, voltage controlled mode] at a fixed temperature ($\sim 20 \text{ K}$), for a sample cooled in zero applied voltage (ZVC)

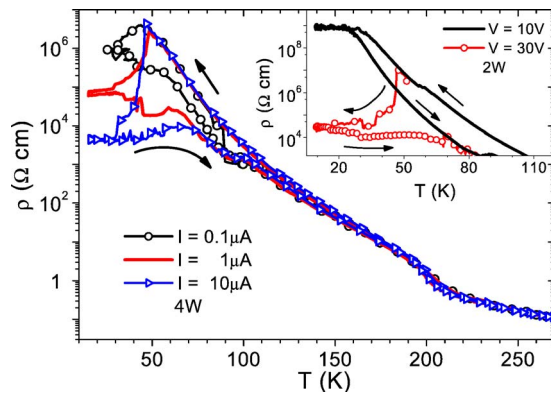


FIG. 1. (Color online) Resistivity (4W, current controlled mode) of LPCMO as a function of temperature for various applied currents. The temperature evolution is indicated by arrows. The inset shows the resistivity obtained in a 2W, voltage controlled mode.

and in a ZFC configuration. A very high and constant resistivity (HR) is measured as the voltage is increased up to a temperature-dependent critical value [$V_c(T)$], where a drop of more than four orders of magnitude is observed. This critical or breakdown voltage depends linearly on the increasing rate of the applied voltage. At this point, a time evolution of the resistivity is observed, which can be easily noticed by the reduction of the resistivity at a constant voltage $V_c(T)$. When the voltage is then decreased, the sample follows a different and more conducting path (LR), eventually reaching the same initial resistivity for low voltages. If the voltage is increased again, memory effects are observed, as the resistivity remains in this LR path [even changing the voltage sign, and for voltages up to $-V_c(T)$], showing a voltage reversible behavior (inset of Fig. 2) and a T^2 temperature dependence (not shown here). Similar results were obtained for temperatures $T \leq 50$ K.

The temperature dependence of $V_c(T)$ (2W, voltage controlled mode) for a ZVC-ZVW experiment can be observed in the upper panel of Fig. 3, where the voltage was increased

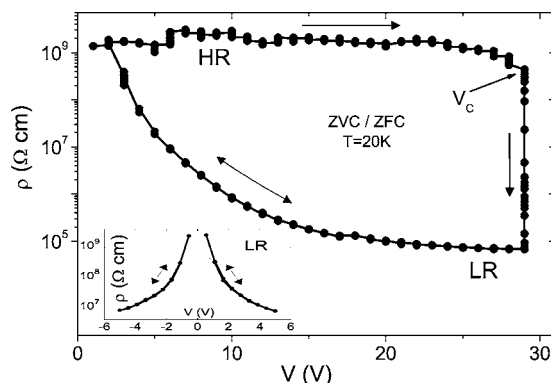


FIG. 2. 2W ZVC resistivity of LPCMO as a function of the applied voltage at $T=20$ K. The system evolves irreversibly from a high-resistance (HR) to a low-resistance (LR) regime, after applying a voltage $V \geq V_c$. Then, independently of the applied voltage, the sample remains in the LR regime until a thermal cycling is performed ($T \geq 70$ K). The inset shows the nonlinear voltage reversible behavior of resistivity in the LR regime.

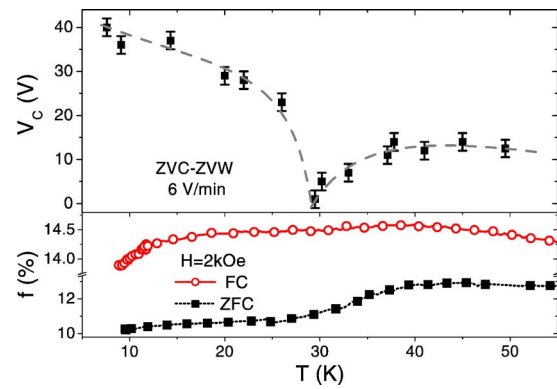


FIG. 3. (Color online) Temperature dependence of the critical voltage (V_c) for a zero-voltage-cooled experiment (upper panel). The lower panel shows the ferromagnetic volume fraction f as a function of temperature in the ZFC and in the FCC modes.

for each case at a 6 V/min rate. In the lower panel, the temperature dependence of the ferromagnetic volume fraction (f) is plotted for comparison. Quite unexpectedly, $V_c \rightarrow 0$ for a temperature ~ 30 K, which is lower than the one corresponding to the maximum of f (~ 40 K) and can be related to a change in the slope of the ZFC magnetization curve.

Joule heating can be an artifact of these $\rho(V)$ measurements,¹²⁻¹⁴ principally when the sample reaches the LR regime and the current considerably increases, flowing mainly in a less resistive metallic percolation path. In this case, the shape of the highest-voltage parts of these $\rho(V)$ curves can be modified by overheating. To rule out this possibility, in particular for $V \leq V_c$, we performed pulsed $\rho(V)$ measurements in the LR regime. As it is shown in Fig. 4, no time dependence can be observed for pulsed and dc voltages up to $V < 10$ V, which can be interpreted as a lack of an overheating contribution to the shape of these $\rho(V)$ characteristics. Thus, as no relevant Joule dissipation can be expected in the HR regime ($\sim 10^4$ less dissipative than LR for $V \sim V_c$), the transition from HR to LR cannot be an overheating artifact.

In these conditions ρ decreases intrinsically with increas-

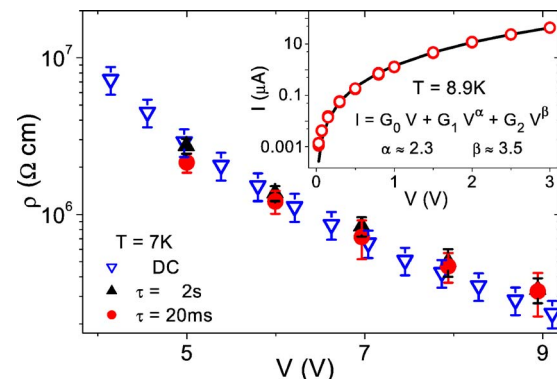


FIG. 4. (Color online) $\rho(V)$ curves measured in the LR regime by applying single square pulses of different time width ($\tau=20$ and 2000 ms) compared to dc measurements. The inset shows the particular $I(V)$ characteristics of the LR regime.

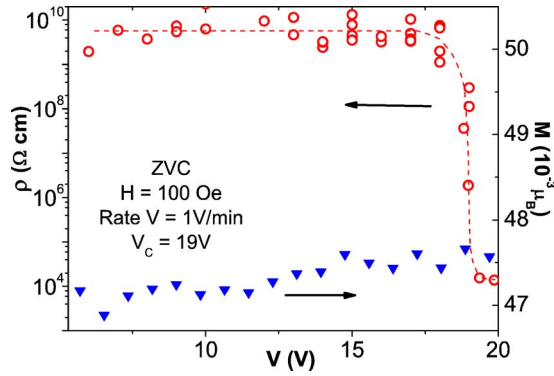


FIG. 5. (Color online) Simultaneous measurements of the voltage dependence of the resistivity and the magnetization in a zero-voltage-cooled and zero-field-cooled experiment, performed at $T \sim 26$ K. The dashed line is a guide to the eye.

ing V . This nonlinear behavior in the LR regime also shows a particular power law dependence of the current (I) on voltage ($I \sim aV + bV^{7/3} + cV^{7/2}$, as shown in the inset of Fig. 4). This behavior was previously observed in analyzing the electrical transport properties through grain boundaries in manganites^{15–18} and was interpreted within the framework described by the Glazman-Matveev theory,¹⁹ which characterizes the case of multistep tunneling of localized states within the grain boundary between two ferromagnetic conducting regions. The tunneling nature of the conducting process derived from our results indicates that the conducting percolation path established in the LR regime is not singly connected.

In order to gain insight about the evolution of f upon the application of a voltage $V > V_c$, we have measured simultaneously $\rho(V)$ and $M(V)$ at low magnetic fields ($H = 100$ Oe). Our results, obtained at $T \sim 26$ K, are shown in Fig. 5. Surprisingly, although our magnetic measurement sensitivity let us detect variations in f lower than 1%, no appreciable changes in the magnetization are detected when the voltage produces a large resistivity drop at V_c . This lack of increase of f points toward the development of a filamentary percolation path, generated upon increase of the applied voltage. This scenario is similar to the one usually observed during the dielectric breakdown of an insulator, where conducting defects increase with increasing voltage to finally produce a percolative path.

Another way to reach the same conclusion, namely, that a one-dimensional (1D) CD-F percolative path is established when the resistivity drop is observed (instead of a 2D or 3D network with an f higher than a critical percolation value f_c), comes from the analysis of ρ measurements by using the general effective medium (GEM) equations developed by McLachlan²⁰ to describe the electric conductivity of a binary mixture of conducting and insulator materials. Within this GEM framework, both 2D and 3D percolation scenarios yield a variation of more than 4% in f when the sample passes from the HR to the LR regime at $V_c(T)$ ($T < 33$ K).²¹ This variation of the ferromagnetic fraction should be easily noticed in the $M(V)$ measurements, which was not the case, confirming the filamentary spatial distribution of the percolating path.

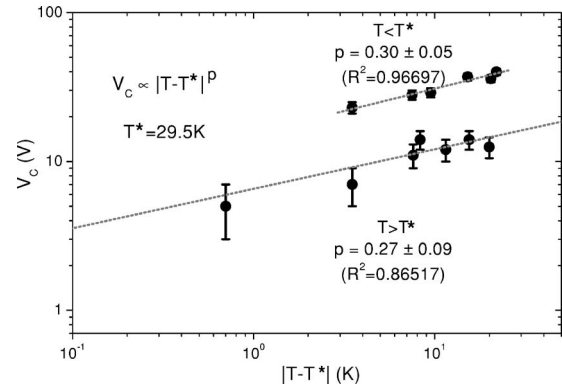


FIG. 6. Critical electric field as a function of the absolute relative temperature $t = |T - T^*|$. The critical exponent $p \approx 0.3$ and $T^* \approx 29.5$ K are obtained from the best fits represented by the dotted lines.

The PS scenario at low temperatures for this prototypical manganite, which can be depicted as small and isolated CD regions in a CO matrix, recalls the physics observed for dielectric breakdown in metal-loaded dielectrics.²² These materials were built as a mixture of a small fraction of a conducting component in an insulating matrix, which is an artificial representation of the intrinsic PS regime observed in manganites. Their dielectric breakdown field (V_{bd}), related to a series of microscopic failures, depends on the conducting volume fraction, as described by an empirical relation of the form

$$\frac{1}{V_{bd}(T)} = A(f) + (f_c - f)^{-\nu} \ln(L), \quad (1)$$

where A is a parameter, f_c the percolation threshold, ν a critical exponent (~ 0.85 in 3D),²³ and L the linear dimension of the sample.

According to Eq. (1) and from the temperature dependence of f obtained from the ZFC magnetization measurement, it is easy to notice that the expected V_{bd} should essentially follow the soft temperature variation of the ZFC magnetization and will not show, in any case, the quite unusual temperature dependence of V_c (shown in Fig. 3). This fact reveals the existence of another process, probably associated with an increase of the dielectric constant (ϵ) that may enhance considerably the local electric field [$V_{bd} = \epsilon(T)V_c(T)$]. Indeed, $V_c(T)$ was found to follow a critical behavior, described by a $|T - T^*|^p$ dependence, as can be observed in Fig. 6. The best fitting parameters correspond to the temperature $T^* \approx 29.5$ K and to the critical exponent $p \approx 0.3$.

Neglecting the small temperature dependence of V_{bd} , as $\epsilon \sim V_c^{-1}$, the obtained critical exponent may correspond to a divergence of ϵ with a critical exponent $p_\epsilon = -p \approx -0.3$. This particular divergence of ϵ was previously observed for binary liquid mixtures near the consolute critical point and can be associated with the Maxwell-Wagner effect.^{24,25} This effect, related to the low-frequency dielectric constant, results from the accumulation of conducting charges at the interface in the boundary between two phases of different conductiv-

ity. The effect is amplified near the consolute point, as the system, which behaves as homogeneous far below this critical temperature, becomes heterogeneous (phase separated) for temperatures above T^* , with the occurrence of large-size phase fluctuations in a critical region. Remarkably, this framework seems to match very well with the PS scenario of manganites, where the CD-F and CO-AF phases coexist in a determined temperature range. In our particular case, below T^* parts of the CD-F and CO-AF phases become miscible, in accordance with the observed ferromagnetic volume fraction reduction, and show large fluctuations between phase-separated and fully mixed (paramagnetic) volumes in a critical region near T^* . These CD-F volume fluctuations favor the formation of a percolation path when applying an external electric field, thus reducing the value needed to reach the critical field [$V_c(T^*) \rightarrow 0$ V].

Recently, Ghivelder *et al.*¹⁰ showed, for this particular manganite, the existence of a boundary between dynamic and frozen PS effects, with a peak in the magnetic viscosity at a temperature pretty close to T^* . By similarity with the binary liquid mixtures, our results may indicate that the reported change in the PS dynamics can be explained by the appearance of this consolutelike point that should produce anomalies in many static and dynamic properties at T^* , as a consequence of the large fluctuations developed near that critical temperature.²⁶

In conclusion, we have shown that the low-temperature

electrical resistivity of LPCMO single crystals is very sensitive to the magnitude of the applied electric field. The resistivity of a zero-electric-field-cooled sample can be varied by more than four orders of magnitude by increasing the exciting voltage over a temperature-dependent critical value [$V_c(T)$]. Our simultaneous electric and magnetic measurements indicate that a filamentary percolation path is established when the resistivity evolves irreversibly from a high- to a low-resistivity regime. The nonlinear I - V characteristics obtained point to the formation of a non-singly connected path where multitunneling processes determine the electric transport properties of this regime. The presence of a consolutelike point at T^* was established by analyzing the critical behavior of V_c , which we associate with a Maxwell-Wagner effect. Thus, the presence of a consolute critical point sheds light on the way that PS occurs, determining the particular behavior of the properties observed for this compound near the critical temperature.

Partial financial support from UBACyT Grant No. X198, ANPCyT PICT Grant No. 03-13517, and CONICET PIP Grant No. 5609 is acknowledged. Work at Rutgers was supported by NSF Grant No. DMR-0520471. G.G., C.A., and P.L. acknowledge financial support from CONICET of Argentina. We are indebted to G. Pasquini for a critical reading of the manuscript.

*Author to whom correspondence should be addressed. Electronic address: acha@df.uba.ar

¹A. Asamitsu, Y. Tomioka, H. Kuwahara, and Y. Tokura, *Nature (London)* **388**, 50 (1997).

²P. Levy, F. Parisi, G. Polla, D. Vega, G. Leyva, H. Lanza, R. S. Freitas, and L. Ghivelder, *Phys. Rev. B* **62**, 6437 (2000).

³V. Hardy, A. Wahl, and C. Martin, *Phys. Rev. B* **64**, 064402 (2001).

⁴N. A. Babushkina, A. N. Taldenkov, L. M. Belova, E. A. Chistotina, O. Y. Gorbenko, A. R. Kaul, K. I. Kugel, and D. I. Khomskii, *Phys. Rev. B* **62**, R6081 (2000).

⁵N. K. Pandey, R. P. S. M. Lobo, and R. C. Budhani, *Phys. Rev. B* **67**, 054413 (2003).

⁶N. A. Babushkina, L. M. Belova, D. I. Khomskii, K. I. Kugel, O. Y. Gorbenko, and A. R. Kaul, *Phys. Rev. B* **59**, 6994 (1999).

⁷M. Uehara, S. Mori, C. H. Chen, and S.-W. Cheong, *Nature (London)* **399**, 560 (1999).

⁸J. Stankiewicz, J. Sesé, J. García, J. Blasco, and C. Rillo, *Phys. Rev. B* **61**, 11236 (2000).

⁹V. Markovich, E. S. Vlahov, Y. Yuzhelevskii, B. Blagoev, K. A. Nenkov, and G. Gorodetsky, *Phys. Rev. B* **72**, 134414 (2005).

¹⁰L. Ghivelder and F. Parisi, *Phys. Rev. B* **71**, 184425 (2005).

¹¹H. J. Lee, K. H. Kim, M. W. Kim, T. W. Noh, B. G. Kim, T. Y. Koo, S.-W. Cheong, Y. J. Wang, and X. Wei, *Phys. Rev. B* **65**, 115118 (2002).

¹²S. Mercone, R. Frésard, V. Caignaert, C. Martin, D. Saurel, C.

Simon, G. André, P. Monod, and F. Fauth, *J. Appl. Phys.* **98**, 023911 (2005).

¹³J. Sacanell, A. G. Leyva, and P. Levy, *J. Appl. Phys.* **98**, 113708 (2005).

¹⁴B. Fisher, J. Genossar, K. B. Chashka, L. Patlagan, G. M. Reischer, and E. Shimshoni, *Appl. Phys. Lett.* **88**, 152103 (2006).

¹⁵J. Klein, C. Höfener, S. Uhlenbruck, L. Alff, B. Büchner, and R. Gross, *Europhys. Lett.* **47**, 371 (1999).

¹⁶C. Höfener, J. B. Philipp, J. Klein, L. Alff, A. Marx, B. Büchner, and R. Gross, *Europhys. Lett.* **50**, 681 (2000).

¹⁷R. Gross *et al.*, *J. Magn. Magn. Mater.* **211**, 150 (2000).

¹⁸K. B. Chashka, B. Fisher, J. Genossar, L. Patlagan, G. Reischer, and E. Shimshoni, *Phys. Rev. B* **63**, 064403 (2001).

¹⁹L. I. Glazman and K. A. Matveev, *Sov. Phys. JETP* **67**, 1276 (1988).

²⁰D. S. McLachlan, *J. Phys. C* **20**, 865 (1987).

²¹G. Garbarino, M. Monteverde, C. Acha, P. Levy, M. Quintero, T. Y. Koo, and S. W. Cheong, *Physica B* **354**, 16 (2004).

²²P. D. Beale and P. M. Duxbury, *Phys. Rev. B* **37**, 2785 (1988).

²³J. W. Essam, *Rep. Prog. Phys.* **43**, 53 (1980).

²⁴J. Thoen, R. Kindt, W. V. Dael, M. Merabet, and T. K. Bose, *Physica A* **156**, 92 (1989).

²⁵J. Hamelin, T. K. Bose, and J. Thoen, *Phys. Rev. A* **42**, 4735 (1990).

²⁶P. C. Hohenberg and B. I. Halperin, *Rev. Mod. Phys.* **49**, 435 (1977).